

Research Paper

Investigation of a Lodged Bullet inside a Human Brain using Computed Tomographic (CT) Imaging

Wubante Mehari Wollelaw¹, Getasew Admasu Wubetu^{2,3*}, Getnet Yitayew Tessema⁴

¹Department of Physics, College of Natural Science and Computational, Debre Markos University, Debre Markos, Ethiopia

²Department of Physics, College of Science, Bahir Dar University, Bahir Dar, Ethiopia

³Department of Physics, College of Natural and Computational Science, Addis Ababa University, Addis Ababa, Ethiopia

⁴Department of Radiology and Imaging, College of Medicine and Health Science, Bahir-Dar University, Bahir Dar, Ethiopia

Article Info

Article History:

Received 02 August 2022

Received in revised form
09 December 2022

Accepted 12 December
2022

Keywords:

Lodged Bullet Investigation,
Computer Tomography,
Attenuation Coefficient,
Hounsfield Value,
X-ray Tomography,
CT Brain Imaging

Abstract

We reported the location of a lodged bullet inside a human brain from the 2D and 3D images using Computed Tomography (CT). It is based on the scanning of the hard and the soft tissues of the brain as well as a bullet by X-ray photons on the circular 3600 CCD detectors. The absorption on the target brain and the bullet had significant differences in the measured current (mA) and the mapped Hounsfield Unit (HU) as a function of the number of slices. The 2D and the reconstructed 3D images displayed the brain soft tissue, which was dark with low HU compared to the white in the bullet part with a higher HU. The attenuation coefficients of a bullet with Copper (Cu) and the skull of the brain with Calcium (Ca) were higher than that of the brain soft tissues with Hydrogen (H) and Oxygen (O). A typical example is the observation of the image at the center of the slices displayed brighter at 3071 HU. 3D structures of brain images were generated and visualized in different viewing positions. The measured value for a lodged bullet was 11.28 cm away from its entry (Frontal), 7.92 cm from the back, and 6.96 cm deep, down from the upper part of the brain. Based on our analysis, the bullet is located in the left hemisphere, which is part of the hypothalamus and parity.

1. Introduction

Computed Tomography (CT) scan is one of the diagnostic tools used to diagnose a patient with a foreign metallic body inserted in the brain. It can image cross-sections with a series of X-ray projections taken from different angles around the patient and captured by the detectors (Landis and Keane et al., 2010). The new design of CT has a revolutionary impact on clinical practice and investigation in forensic medicine for the observation of foreign bodies embedded in a person (De Beer et al., 2008). CT imaging is a highly acceptable method of investigating a lodged bullet inside the

human brain (Gascho, 2021; Bolliger, 2021; Thali, 2021a). The CT has high spatial resolution and detections at different angles for taking the capture of different slices of 2D images and later building them up to the reconstructed 3D images (Liu, 2022; Gascho et al., 2020). Previous studies have shown that CT allows accurate detection and classification of foreign metals such as cardiac pacemakers, ferromagnetic vascular clips, and nerve simulators (Nguyen et al., 2017). The detection of a bullet inside the brain has been studied by different authors such as Gascho et al., (2020). X-ray

*Corresponding author, e-mail: getasew.wubetu2@mail.dcu.ie or getasew.admasu@bdu.edu.et

<https://doi.org/10.20372/ejssdastu.v10.i1.2023.531>

radiation can cause permanent damage to a brain during scanning so proper dose and careful detection are needed (Gascho, 2020b; Bolliger, 2021b and Thali, 2021b). Such detection can help to look at the hidden part of the brain with inserted metal as the attenuations of the metals; these attenuations of metals are different: the hard and soft tissues of the brain (Bolliger and Thali, 2021b). It has been observed from the 2D and the reconstructed 3D images that the attenuation coefficient of Cu is greater than that of Ca and soft tissues (Seletchi and Dului, 2007).

In this work, we investigated a lodged bullet inside the dead body of a 25-year-old man using CT imaging. The 2D images were taken from Felege Hiwot Referral Hospital and the reconstructed 3D images from the 2D images by radiant viewer software. Then, the location of the bullet in the brain was determined quantitatively and qualitatively from the measured current values. It is derived from the attenuation of the incident X-ray source detection on both the hard and soft tissues of the brain as well as the bullet in the form of the measured current and the mapped HU.

2. Materials and Methods

2.1. Instrumentation

Figure 1 displays the Optima CT-540 scan machine at Felege Hiwot Specialized Hospital in Bahir Dar, Ethiopia. This machine has three main parts: an X-ray source, detectors, and a circular sample stage. The X-ray source was rotated through the gantry and equipped with 3600 detectors in a circular ring-like structure. Standard imaging protocols were used to image the bullet embedded in the brain of the dead body of a 25-year-old man who died by a gunshot. The key input parameters were set for the CT scan with a peak voltage of 120 kV, current scout image of 10 mA, slice thickness of 0.625 mm, scanning time of 2s, and the helical acquisition protocol. The data acquisitions were taken step-by-step for measuring the 2D images at different projections.

2.2. Imaging Procedure

In the imaging process, the first thing is to keep the patient inside the Gantry on the CT scan and lay him down on the examination table in the appropriate position. The X-ray beam was focused onto the brain of the dead body of a man that follows a spiral path of rotation to be imaged by each 3600 CCD detector in the

circular directions. The input parameters were set with a low radiation dose to produce quality images. Normally, there is a standard procedure for taking the patient's 2D images by setting the noise management that should be pre-set to filter out unnecessary data to be shielded and set at lower peak voltage settings to accomplish the lowest possible dose necessary. Then, the CT scan was set to measure the cross-sectional images of 2D slices and further constructed the 3D image (Gruetzemacher et al., 2018). Generally, the technologist took the order to the patient to avoid any movement during the scan; hence, this will be important in taking quality images of the examination (Fahrni et al., 2017). The CT computer program process had a large volume of data to create two-dimensional cross-sectional images of a patient's head part which were then displayed on a monitor. Then, the image processing was completed using radiant viewer software. The scout and slices were generated from the CT images taken.

2.3. The Physics of x-ray Computed Tomography

The X-ray radiation depends on parameters such as intensity, attenuation, wavelength, and microstructural parameters of the human brain (Sagsoz et al., 2010). X-ray tomography was used to visualize the hard and soft tissues alternatively (Said, Noor, and Yueniwati, 2014). Appropriate software is used for better efficiency, higher sensitivity, faster exposure, and dynamic imaging (Cong., et al 2011). Figure 2 shows the basic principle that governs the interaction of the X-ray with the sample to give a 2D image projection constructed to the 3D image. Assuming that the X-rays are a single energetic source, the intensity I_1 of an X-ray beam of incident intensity I_0 transmitted beam through a small volume of tissue having thickness x and attenuation coefficient μ_1 (Turbell et al., 2001) can be written based on Beer-Lambert law as:

$$I_1 = I_0 e^{-\mu_1 x} \quad (1)$$

The scanning of the X-rays passes from one side to the other with the Charge Coupled Device (CCD) detection recording the attenuated coefficient for both the bullet and the brain's soft and hard tissues. The intensity of the attenuated X-ray source is given by (Chamard et al., 2010):

$$I = I_0 e^{-\sum_1^n \mu_i x_i} \quad (2)$$

where μ_i and x_i are the linear attenuation coefficient of, and path length through, the material, i .

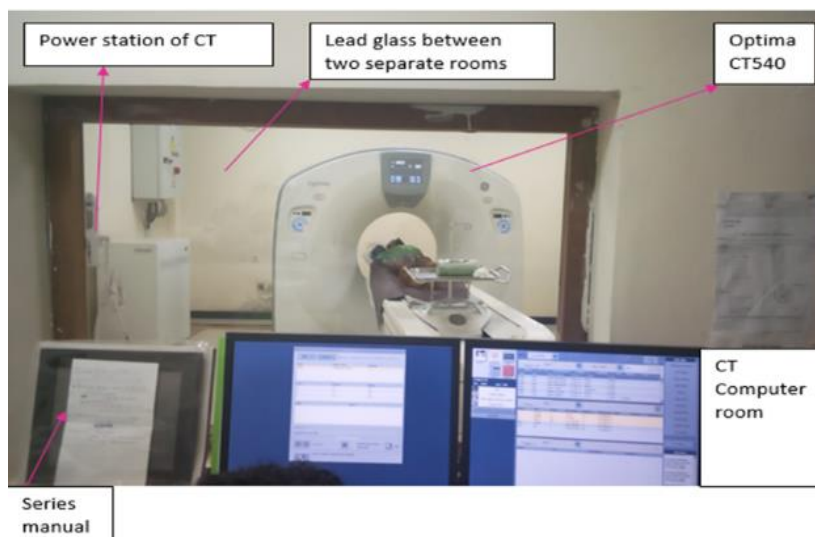


Figure 1: The CT machine is displayed in two separate rooms for medical imaging in Felege Hiwot Specialized Hospital

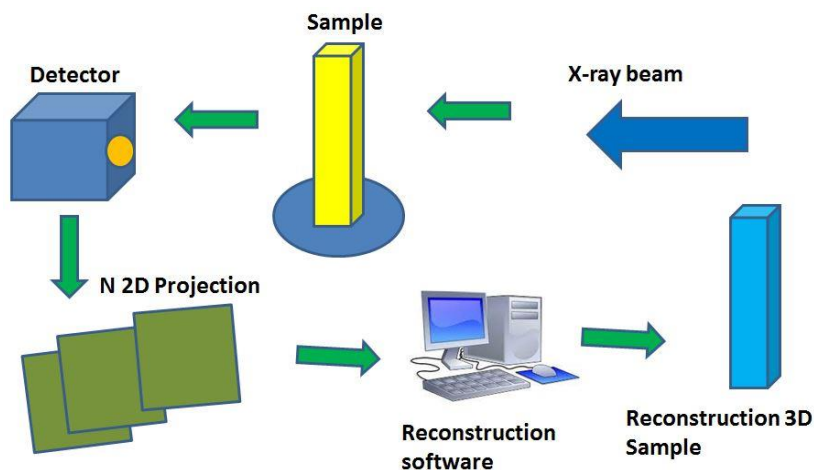


Figure 2: Basic principle of CT imaging procedure to construct the 3D image from 2D slices.

3.Results and Discussion

The CT data are manipulated sequentially in the 2D slices and computationally reconstructed by adding each slice to 3D images. The radiant viewer software is a powerful tool for manipulating the HU values for each slice of the brain with a bullet inside. Three modes of assessment have been used to study the embedded bullet (Xue et al., 2012). These include imaging based on scout images, current properties, and HU values of the slices respectively.

3.1.Scout Images

Figure 3 illustrates the scout image of a head. The frontal and lateral scout images show in A and C respectively with a question mark to identify the

location of the bullet from different directions. As mentioned earlier, the introduction part of the 2D and reconstructed 3D imaging is helpful to extract the measured current in mA and HU as a function of the number of slices from the differences in the intensity (I) the attenuation coefficients of the hard and soft brain tissues and a bullet.

3.2.Image Slices

Figure 4 displays the multiple discrete slices produced using the scout CT scan to define the starting and ending locations of the head. The 255 slice thicknesses were measured to be 0.625 mm generated from the diagnosis of the lodged bullet inside the skull.

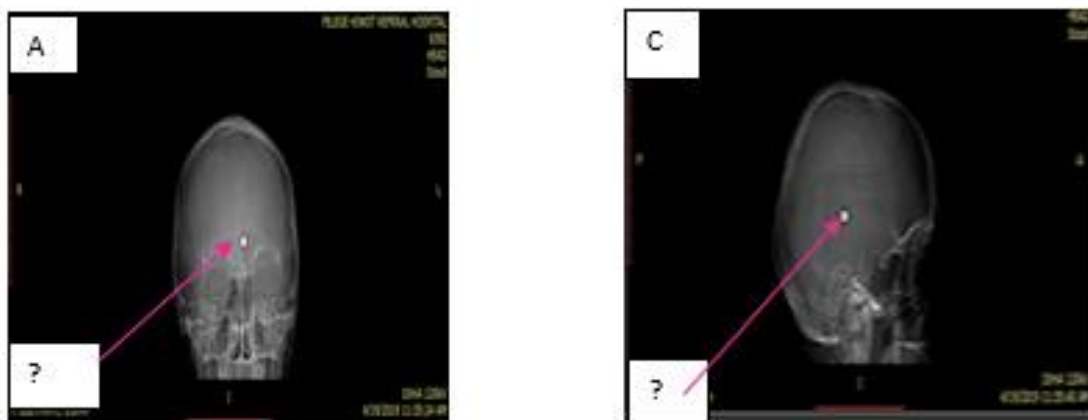


Figure 3: The scout images of a head.

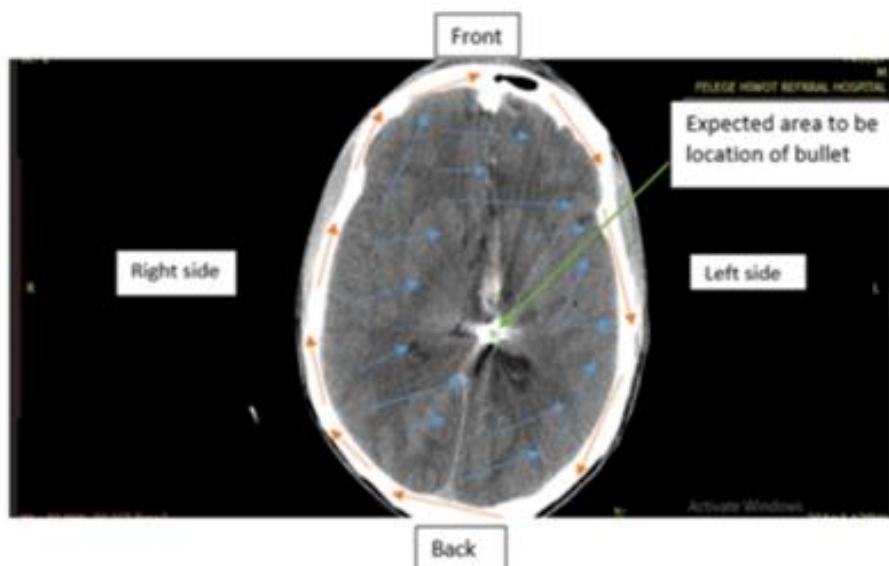


Figure 4: The 2D view of a slice image of the brain with different profiles.

The 2D slices correspond to the gray levels of the images of the head due to X-ray source attenuation, reflection, scattering, and absorption. Typically, the X-ray attenuation primarily is a function of X-ray energy and the density and composition of the brain tissues and the bullet. From the measured HU and current values, it is indicated that the gray level observed by the blue arrows on the 2D slice image of a brain with a different profile of CT imaging for a variation of a slice thickness in a range of 3 to 5 mm (Osborne et al., 2016) and the interpretation based on Michael et al., (2001). The assignment of each pixel based on the attenuation of water value on the scale reading is named Hounsfield Units (HU), after Sir Godfrey Hounsfield (Osborne et al., 2016).

The different tissues are represented by arrows as displayed in Figure 4. Blue arrows indicate air, fat, fluid,

and soft tissue of the brain described as the red dot lines (beam hardening artifact from the metal alloy in a lodged bullet). Besides, the red arrows around the brain (bone of the skull around the brain) display the bright area indicated at the center of the slices by the green arrow that shows the expected location of the bullet in the brain. The CT helical slice above highlights the common anatomical structures which may help interpret the CT image of a shot brain. The HU value ranges of each area indicated using different arrows are labeled in Table 1 based on the following equation:

$$H = \frac{\mu_{water}}{\mu_{tissue}} \times 100 \tag{3}$$

where μ_{water} and μ_{tissue} are the linear attenuation coefficient of water and the linear attenuation coefficient of tissue, respectively.

Table 1: HU values of areas indicated by different arrows and their profiles in Figure 4

Areas indicated by arrows	HU values in (HU)	Remarks
Area indicated by red arrows	768 up to 1434	Skull bone
Area indicated by blue arrows	-15 up to 43	Fluid and Soft tissues
Area indicated by green arrow at the center	3071	Bullet

The amount of X-rays absorbed by the brain and the bullet was mapped as HU. The denser the tissue, the more X-rays were attenuated, and the higher the number of HU. Water was always set to be 0 HU, while the air was -1000HU, and bones had values between several hundred to thousands of HU (Bolliger et al., 2021). Brain profiles were thus separated (air, soft tissues, fluids, bone, and bullets). The HU mapping was in the range of -1024 to +3071 for the CT scan. Therefore, the maximum HU value was determined to be the bullet. The penetration level of the bullet was determined individually from the measured slice variation in both brightness and darkness, as shown in Figure 5. It can be observed that the bright image with a higher density of the bullet has attenuation that only allows a small amount of radiation to pass through it.

Typically, the 108th and 124th slices with a dark area at the center of the 2D slice images have been observed in Figure 5. However, the slices of the 109th to 123rd images have brighter areas at the center that indicates a lodged bullet in these slice numbers. Therefore, the scan of the X-rays onto the metal bullet highly attenuated the incident source due to the heavier metallic atoms Cu in the bullet. Besides, the observation of a brain with a higher elemental combination of water of H and O atoms is observed as dark, there are heavy elements Ca for the hard tissue and Cu for a bullet with brighter figure print in the 2D slices each slice as a brighter area.

3.2.1. The current (in mA) through the slices

Figure 6 (a) displays the variation of the measured current vs. the number of slices set in the brain. The incident current was set at 10 mA and it produces 100 to 306 mA for each slice. It has been observed that the maximum current was recorded in the range of 300 to 306 mA for the slice numbers ranging from 100-120. It has been observed that such a high current for these slices is due to the presence of a bullet in the scanned slices that increases the conductivity of the measured slice and in turn, increases the current in these ranges of the measured slices. The variation of 255 slices with

constant readings of the current was assessed on the slices between the 105th and 123rd. The brain profiles are composed of different materials. So Cu in a bullet is a conductor with low resistivity. So, slices that had a bullet read the high current value. The current readings on the other slices were controlled by a high resistance of the brain profiles. The current readings from slices 105th up to 123rd were constant as a result of the presence of the bullet. A maximum of 306 mA current was measured from the 2D images of slices as the result of the higher conductivity of Cu in a bullet. However, the currents were normal for the 2D I slices that varied from 112 mA up to 304 mA.

3.2.2. The Hounsfield value profiles of the slices

Studies prove that metal artifacts degrade the image qualities of bullets (Makris et al., 2008). In contrast, the results of 2D image slices measured as HU were displayed in Figures 6 (b) as the results of the different densities in a head such as air, water, soft tissue bone, hard tissue, and a bullet in terms of different HU values. Medical scanners typically work in a range of -1024 HU to +3071 HU (Osborne et al., 2016). It is labeled as the tissues greater than +100 HU in density appears pure white. There are standard labels in HU, where fat (-60 HU) and air (-1000HU) respectively form the examined patients. Therefore, in this work, the HU value reading includes the maximum range of the medical scanner, the same +3071 HU (pure white), where a lodged bullet is identified. Some slice profiles were assessed as Cerebrospinal fluid (CSF) (0 HU), Skull bone (+100 HU), fat (-50 HU), the air outside the patient (-1000 HU), and subdural hematoma (+60 HU) (Gigantesco and Giuliani, 2011). We discussed the image profiles of the slices based on the HU values by plotting the graph as shown in Figure 6(b). This assessment included 22 slices. The HU numbers were closely spaced at the ranges of the soft tissue and below the level of water. Spatially, slices from 111th up to 120th indicated the HU values around the proposed range.

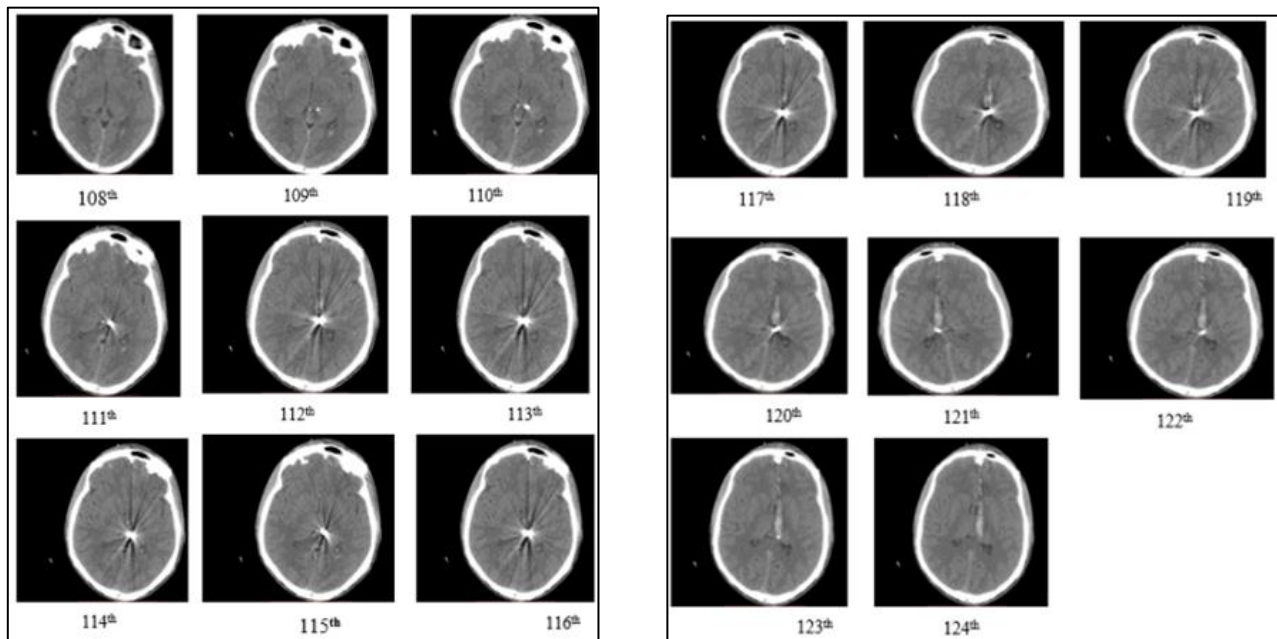


Figure 5: Systematic illustrations of slice images of the head (from 108th up to 124th).

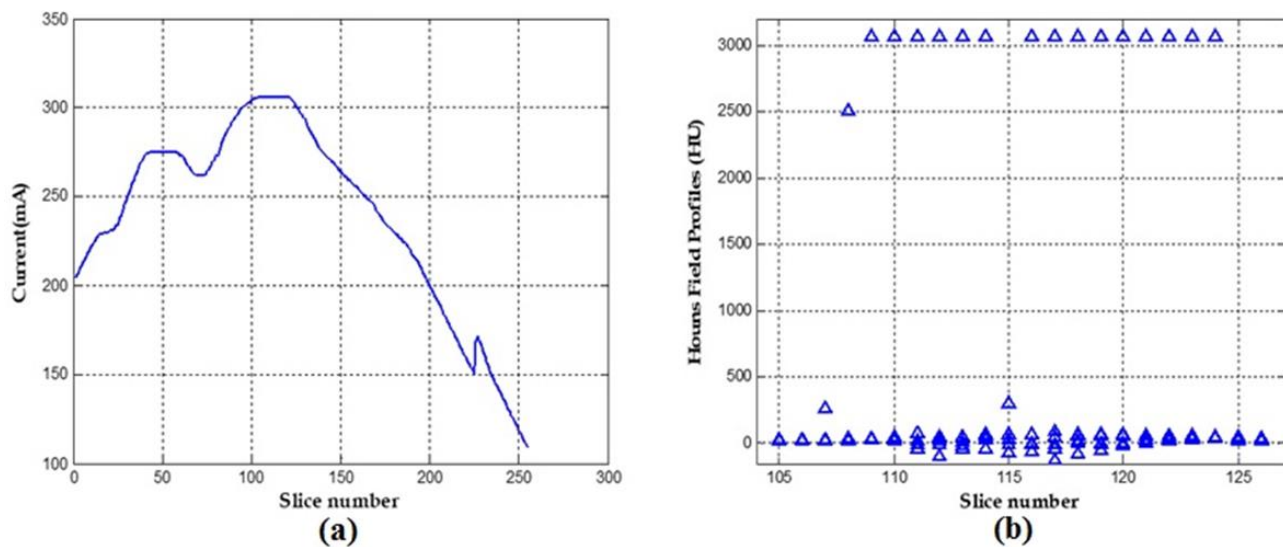


Figure 6 (a): The tube current vs. number of slices; (b): The HU values as a function of the number of a slice with maxima and minima in HS.

The center of the selected slices was evaluated as 3071 HU (pure white) and slices from 111th up to 121th had closely spaced HU readings below the level of water. Most of the indicated areas of the slices indicate that the profile around the location of the proposed area might be soft tissues and fluid. It has been observed that the 3071 HU was at the center of the measured slices to the 109th to 123rd. Now, the HU values through the brain images were compared with previous literature and discussed accordingly. It is believed that the CSF HU values are in

the range of 0 to 15 (Nguyen et al., 2017). The HU ranges could vary from -1000 HU (air) up to +1000 HU (metal) (Makris et al., 2008). The range of CT scan numbers was at HU value of up to 2000, and each scan represents a shade of gray with +1000 (white) and -100 (black) at either end of the spectrum. It has been indicated by (Gruetzemacher and Paradice, 2018), the metals' HU values are above 1000HU. However, the image of the bullet could read 3071 HU. CT scan 2D slices at different levels can determine the ventricular system with a central

image depicting the CSF flows. It has a lateral ventricle and CSF circulates into the subarachnoid space by exiting through the medial and lateral apertures (Lind et al., 2019).

3.2.3. The location of a lodged bullet

The internal structure of the brain around the location of a lodged bullet is indicated as the lateral cerebral vein, third ventricle, lateral ventricle, internal cerebral veins, midbrain, cerebral aqueduct, and thalamus. We investigated a lodged bullet at the left side of the third ventricle. The helical slice of the brain parts around the lodged bullet is shown in Figure 7 (a).

The 3D multiple planar reconstructions (MPR) technique was preferred to compare 2D and 3D images of the brain. The 3D MPR images of the brain were displayed and appropriate positions were adjusted by locating the x-y coordinate system at the location of the lodged bullet on slices. In this setup, the frontal and lateral 3D images and the selected slices were displayed at the same time. The comparison between 2D and 3D images helped guess and investigate the location of the lodged bullet inside the brain, as shown in Figure 7 (b).

We compared the lateral and frontal 3D images with 2D slices to gain evidence about the location of the bullet. The slices and the frontal 3D images indicated as the bullet was located in the left hemisphere of the brain. The lateral 3D image of the brain demonstrated how much the location was deep and how far the bullet was from the entry part at the frontal.

The lengths were 11.28cm from the frontal, 79.2cm from the back, 6.96cm from the upper part of the brain, and as far as possible from the area of the mouth to the location of the lodged bullet respectively, as shown in Figure 8 (a). The bullet is closely located on two major parts of the brain, namely, the Hypothalamus, which is the central part of the brain, and the Parietal, which is part of the Cerebrum.

The use of CSF selection as a reference may serve as an adjunct for the evaluation of surgical lesions (Kurihara et al., 2013). The CSF refers to the space between the dura and the pia mater (Papp et al., 2017). This space is filled with cerebrospinal fluid, which is a clear, very low-protein liquid similar to blood plasma but with a different electrolyte concentration (Nguyen et al., 2017). This system is divided into two to four

cavities that are connected by a series of holes. Two ventricles are enclosed in the cerebral hemisphere called lateral ventricles which could be part of the location of the bullet. CSF volume is the nearest and comparable to a lateral ventricle (Osborne et al., 2016).

The CT scan imaging was taken by the CCD to image the 2D slices, which were later constructed by the 3D images as shown in Figure 8 (b). CT scan imaging changes the modern approach to determining patients' practical observation of the brain that pre-determines to acquire 0.5 to 0.625 mm thick tomographic images (Ro et al., 2015). In this work, we set the slice thickness at 0.625 mm to include the region of interest to investigate the location of the bullet, as shown in the reconstructed 3D image shown in Figure 8 (b).

3.3. Three-dimensional (3D) images

The 3D images of the head anatomy and the surrounding structures can be based on the interpretation of 2D slice summations (Osborne et al., 2016). It is based on the generation of 2D images using radiant viewer software. Such visualization can help to determine the small thickness in the measured multiple slices. It has been observed that a lodged bullet was on the 17 slices (ranging from 108th up to 124th) from the generated 3D image and is found to be 10.625 mm thick. The gray and dark colors help us to determine the HU for these measured slices. The upper gray level is measured at 1450 HU and the lower one at -900 HU. The darker colors range from -900 to 1450 HU. However, the upper gray levels are in the range of 1450 to 3071 HU for the brighter part touched by a bullet.

Figure 9 shows the frontal view of the head with an observation of the point link in the front skull and observed a lodged bullet from the reconstruction of the 255 slices. The bullet entered the skull at the front of the head and there was no indication of an exit wound, so the bullet may remain inside the head. Here, the image has WW: 287, WL: 332, L-I: 0.00, S-I: 210 HU. This means that a total range of 287 HU is displayed, centered on a density of 332 HU. Figure 9 (a) shows a 3D image generated from 255 slices of 2D images. The original 3D image was rotated at 210 ... towards a vertical ... with the best number of selected slices based on their physical profiles to map the skull.

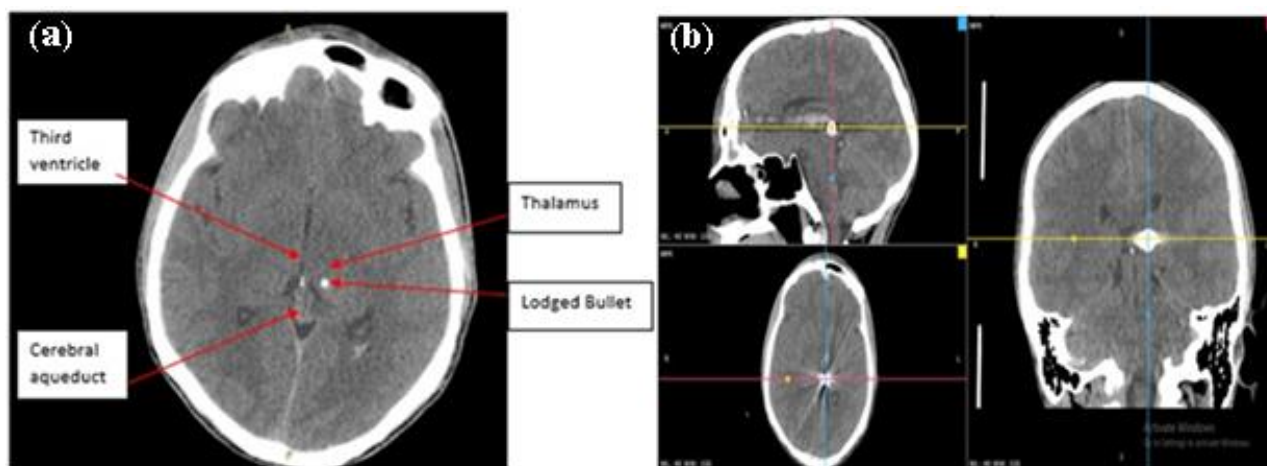


Figure 7 (a): Illustration of helical slices of brain parts around the location of a lodged bullet; (b): Comparison of a lodged bullet location using 2D and 3D images.

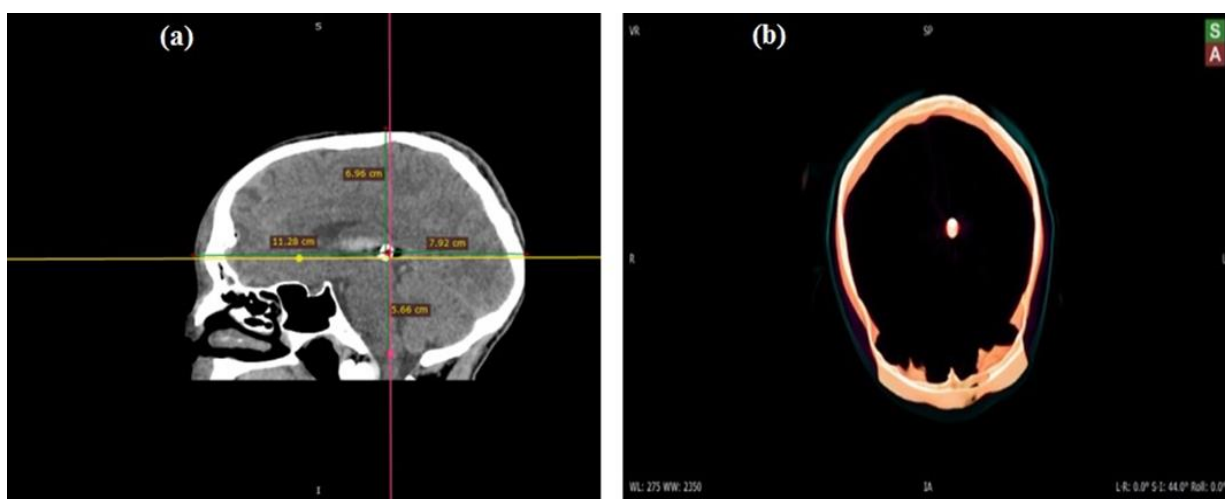


Figure 8; (a) Illustration of the location of the bullet from the 3D MPR method; (b) 3D image generated from 17 slices.

The visualization of the internal parts of the head was shown from the deeper upper layer to the hypothalamus by rotating the 3D images at different directions and angles. This 3D image of the skull shown in Figure 9 (b) was constructed from the first 200 slices out of 255 that generate a slice thickness of 0.625mm. Our brain has complex structures and different functions. The images are displayed with the parameters such as WL at 287, WW at 332, LR at 00, SI at 63.40, and Roll at 21.80. This means that a total range of 287 HU is displayed, centered on a density of 332 HU. The 3D image was constructed from 200 slices and rotated at 70.00 towards a vertical circular trajectory downwards to observe the location of the lodged bullet inside the 3D image of the brain. This

image could show the location of the bullet in the internal part of the brain, around the hypothalamic area. To be sure about the location of the lodged bullet in the hypothalamic part, the rotated images are shown in Figure 10.

To further observe the reconstructed 3D images at different angles upon the rotation of the X-rays, the source in the Gantry is shown in Figure 9 and Figure 10. The visualization of the 3D images displayed taking B_0 as referenced is anticlockwise rotated by B_1 by 700, B_2 by 800, and B_3 by 850 HU respectively. The findings of this study show that the bullet has traveled subcutaneously through the cerebrum passed through the lateral ventricle, and rested in the hypothalamus, near the cerebellum.

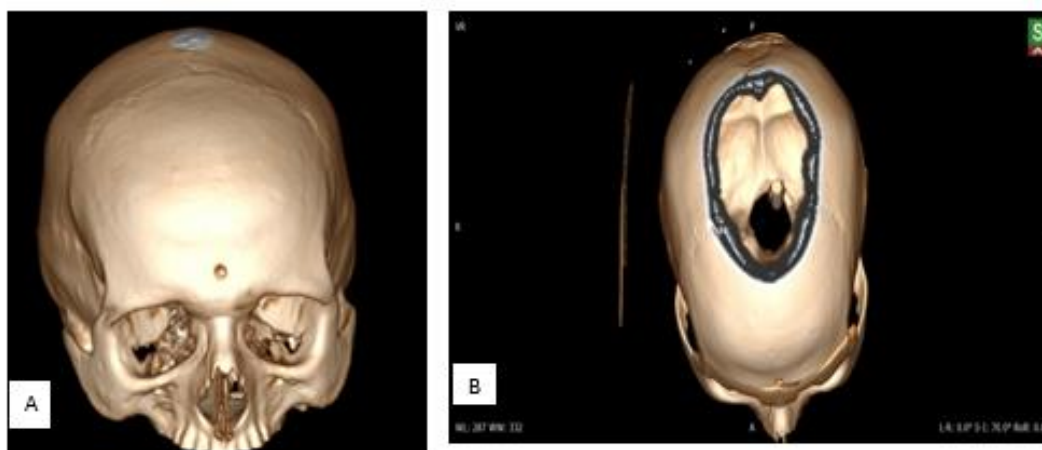


Figure 9: Illustration of 3D CT image of skull very well demonstrating entry of the lodged bullet.



Figure 10: Systematic visualizations of the location of the bullet in different viewing positions.

4. Conclusion

The clear observation of an embedded bullet can be easily identified by taking successive 2D slices by the CT scan and later reconstructing it into 3D images using radiant software. The X-ray source is scanning both the hard and soft tissues of the brain and an embedded bullet. The attenuation coefficients are different for these targets. It is based on the differences in the intensities for the measured values for the air, water, soft and hard tissue, and a bullet during the 2D slices images to measure the current in mA for each slice and mapped to the HU. Typically, the HU value of the bullet was 3071H. The current readings from the slices were maximum on the lodged bullet due to the high density of the bullet made of Cu and low current flows through normal slices made of H & O (slices without a bullet). The 3D images were rotated in different positions to visualize the bullet inside the brain images. Correspondingly, findings from scout

images, slices, and 3D images indicate that the bullet entered the frontal skull, and then passed toward the frontal cerebrum and other complex parts of the left hemisphere of the brain. Finally, the lodged bullet is estimated to be in the ventricular system and the hypothalamus part of the brain image. An experienced physician could refer to this type of study during medical and surgical cases. Atypical gunshot wounds, such as the case under investigation, an implications for multiple issues including delayed diagnostic tests, inaccurate radiological readings, and inappropriate medication management. Ordering full head CT scans and making quick decisions in surgical and medical management are critical takeaways in providing quality care to patients with these injuries.

Acknowledgment

The authors would like to thank Bahir Dar University, Ethiopia, for providing a scholarship to the first author to complete his MSc research in Laser Spectroscopy.

We also extend our gratitude to Felege Hiwot Specialized Hospital, Bahir Dar, Ethiopia, for providing us with the CT data.

Conflict of Interest

On behalf of all authors, the corresponding author declares that there is no conflict of interest in this study.

Authors' Contributions

GAW has proposed the problem and GY has provided the CT images. WMA and GAW have processed the CT images to convert the physical parameters and interpret the data. WMW has drafted the manuscript and GAW reviewed the manuscript. All of the writers have approved the manuscript in its current state.

Ethical Statement/Consent

The authors declare that there is no human participant in the investigation of our paper. The experiment result was based on the CT imaging of the body of a 25-year-old person to look at the physics of a lodged bullet inside the human brain. Therefore, the authors declare that the work described has been carried out following the Declaration of Helsinki of the World Medical Association revised in 2013 for experiments involving humans as well as following the EU Directive 2010/63/EU for animal experiments.

Reference

- Chamard, V., Stang, J., Carbone, G., Diaz, A., Chen, G., Alfonso, C., Mocuta, C. and Metzger, T. H. (2010). Three-Dimensional X-Ray Fourier Transform Holography: The Bragg Case. *Phys. Rev. Lett.*, 104(16): 165501. <https://doi.org/10.1103/PhysRevLett.104.165501>.
- Cong, W., Atsushi, M., and Ge., W. (2012). Fourier Transform-Based Iterative Method for X-Ray Differential Phase-Contrast Computed Tomography. *Opt. Lett.*, 37(11):1784-6. doi: 10.1364/OL.37.001784.
- De Beer, F. C., Prevec, R., Cisneros, J., & Abdala, F. (2008). Hidden Structure of Fossils Revealed by Neutron and X-Ray Tomography. *Neutron Radiography*, (8): 452–461
- Fahrni, S., Lorenzo Campana, L., Dominguez, A., Uldin, T., Dedouit, F., Delémont, O., Grabherr, S. (2017). CT-Scan vs . 3D Surface Scanning of a Skull: First Considerations Regarding Reproducibility Issues. *Forensic Sci. Res.*, 2(2): 93–99. <https://doi.org/10.1080/20961790.2017.1334353>
- Gascho, D. (2020). Lodged bullets on computed tomography: Three classification procedures for the virtual investigation of bullets or their fragments that cannot be recovered from the living patient. *Med. Sci. Law*, 60(4), 245–248. <https://doi.org/10.1177/0025802420962697>.
- Gascho, D., Bolliger, S. A., & Thali, M. J. (2021a). CT and MRI of a transcadiac gunshot wound with an annular distribution of bullet fragments surrounding an exit-re-entrance wound after the bullet burst from a floor tile upon exiting the lying body. *J. Forensic Leg. Med.*, 77:102087. <https://doi.org/10.1016/j.jflm.2020.102087>.
- Gascho, D., Bolliger, S. A., & Thali, M. J. (2021b). CT and MRI of a transcadiac gunshot wound with an annular distribution of bullet fragments surrounding an exit-re-entrance wound after the bullet burst from a floor tile upon exiting the lying body. *J. Forensic Leg. Med.*, 77. <https://doi.org/10.1016/j.jflm.2020.102087>.
- Gascho, D., Zoelch, N., Richter, H., Buehlmann, A., Wyss, P., Thali, M. J., & Schaerli, S. (2020). Heavy metal in radiology: how to reliably differentiate between lodged copper and lead bullets using CT numbers. *Eur. Radiol. Exp.*, 4(1). <https://doi.org/10.1186/s41747-020-00168-z>.
- Gigantesco, A. and Giuliani, M. (2011). Quality of Life in Mental Health Services with a Focus on Psychiatric Rehabilitation Practice. *Ann Ist Super Sanità*, 47(4): 363–72. <https://doi.org/10.4415/ANN>.
- Gruetzemacher, R., Gupta, A. and Paradice, D. (2018). 3D Deep Learning for Detecting Pulmonary Nodules in CT Scans. *J. Am. Med. Inform. Assoc.*, 25(10): 1301–10. <https://doi.org/10.1093/jamia/ocy098>
- Kurihara, Y., Yakushiji, Y. K., Matsumoto, J., Ishikawa, T., Hirata, K. (2013). The Ribs: Anatomic and Radiologic Considerations. *RadioGraphics* 19(1): 105–19. <https://doi.org/10.1148/radiographics.19.1.g99ja02105>.
- Landis, E. N. and Keane, D. T. (2010). X-Ray Microtomography. *Mater. Charact.*, 61(12): 1305–1316. <https://doi.org/10.1016/j.matchar.2010.09.012>.
- Lind, A. L., Just, D., Mikus, M., Fredolini, C., Ioannou, M., Gerdle, B., Ghafouri, B., Bäckryd, E., Tanum, L., Gordh, T., Månberg, A. (2019). CSF levels of apolipoprotein C1 and autotaxin found to associate with neuropathic pain and fibromyalgia. *J. Pain Res.*

- 12:2875-2889. <https://doi.org/10.2147/JPR.S215348>.
- Liu, Y., Cui, Y., Yang, C., Cui, C., Jing, D., Zhang, X., Chen, Y., Li, B., Liang, Z., Chen, K., Zhang, Z. and Wu, L. (2022). The Brain Structural and Functional Anomaly Associated with Simultanagnosia in Patients with Posterior Cortical Atrophy. *Brain Imaging and Behav.*, 16:1148–1162. <https://doi.org/10.1007/s11682-021-00568-8>.
- Makris, N., Angelone, L., Tulloch, S., Sorg, S., Kaiser, J., Kennedy, D., Bonmassar, G. (2008). MRI-Based Anatomical Model of the Human Head for Specific Absorption Rate Mapping. *Med. Biol. Eng. Comput.*, 46(12): 1239–51. <https://doi.org/10.1007/s11517-008-0414-z>.
- Nguyen, H. S., Patel, M., Li, L., Kurpad, S. and Mueller, W. (2017). Quantitative Estimation of a Ratio of Intracranial Cerebrospinal Fluid Volume to Brain Volume Based on Segmentation of CT Images in Patients with Extra-Axial Hematoma. *Neuroradiol. J.*, 130(1): 10–14. <https://doi.org/10.1177/1971400916678227>.
- Osborne, T., Christine, T., Kivraj, S. and Vineet, P. (2016). How to Interpret an Unenhanced CT Brain Scan. Part 1 : Basic Principles of Computed Tomography and Relevant Neuroanatomy. *South Sudan Med. J.*, 9(3): 67–69.
- Papp, C., Pak, K., Erdei, T., Juhasz, B., Seres, I., Szentpéteri, A., Kardos, L., Szilasi, M., Gesztelyi, R., Zsuga, J. (2017). Alteration of the Irisin-Brain-Derived Neurotrophic Factor Axis Contributes to Disturbance of Mood in COPD Patients. *Int. J. Chron. Obstruct. Pulmon Dis.*, 12:2023-2033 <https://doi.org/10.2147/COPD.S135701>.
- Ro, T., Richard, M., Dan, G. and Muhammad, H. N. (2015). Atypical Gunshot Wound: Bullet Trajectory Analyzed by Computed Tomography. *Int. J. Surg. Case Rep.*, 14: 104–7. <http://dx.doi.org/10.1016/j.ijscr.2015.07.023>.
- Sagsoz, M. E., Fazli, E., Salih, Z. E. and İhsan, Y. (2010). Determination of Linear X-Ray Attenuation Coefficients of Pathological Brain Tissues and Use of Filters in Tissue Contrast Enhancement in Computed Tomography. *Eurasian J. Med.*, 42(2): 53–56. <https://doi.org/10.5152/eajm.2010.17>.
- Said, S. J., Noor, J. A., and Yueniwati, Y. (2014). Identification of Ischemic Stroke Stages in CT Scan Brain Images Using JImageJ Software. *Int. Refereed J. Eng. Technol (IRJES)*, 3(7): 24–31.
- Seletchi, E.D. and Dului, O. G. (2007). Image Processing and Data Analysis in Computed Tomography. *Rom. J. Phys.*, 52(5–7): 667–75.
- Turbell, H. (2001). *Cone-Beam Reconstruction Using Filtered backprojection*. In *Science And Technology* (Issue 672). doi=10.1.1.134.5224 & amp;rep=rep1&type=pdf.
- Xue, Z., Antani, S. K., Long, R. L., Demner-Fushman, D. and Thoma, G. R. (2012). Window Classification of Brain CT Images in Biomedical Articles. *AMIA Annual Symposium proceedings*. 2012:1023–29.